Polymer Bulletin 53, 393–400 (2005)
DOI 10.1007/s00289-005-0348-7

Polymer Bulletin

Preparation and Characterization of PS/Multi-Walled Carbon Nanotube Nanocomposites

Young-Jin Choi,[1] Seok-Ho Hwang,[2] Yoo Seok Hong,[3] Jang-Yup Kim,[1] Chang-Yul Ok,[1] Wansoo Huh,[1] Sang-Won Lee[1]*

[1] Department of Chemical & Environmental Engineering, Soongsil University, Seoul 156-743, KOREA (*e-mail: lswon@ssu.ac.kr)
[2] Department of Polymer Science, The University of Akron, Akron, OH 44325-3909, USA
[3] R&D Center, Volvik Co., Ltd, Seoul 369-824, KOREA

Received: 25 July 2004 / Revised version: 23 November 2004 / Accepted: 25 January 2005
Published online: 24 February 2005 –

Summary

Nanocomposites of polystyrene (PS) with multi-walled carbon nanotubes (MWNT) were produced by co-rotating twin-screw extruder. Characterization of these materials included scanning electron microscopy (SEM), transmission electron microscopy (TEM) and rheology in order to obtain the information on the dispersion of MWNT in the polymeric matrix. It is found that the MWNT dispersed uniformly through the PS matrix showing no significant agglomeration in the various compositions studied. In addition, we also investigated the thermal properties, glass transition temperature and thermal decomposition behavior as a function of the increasing MWNT content.

Introduction

During the last decade, the intriguing mechanical and physical properties of carbon nanotubes have stimulated intensive research into the development of novel polymer nanocomposites.[1] Generally, the small size of the nano-scale filler should not only ensure a good surface finish but should also improve processability as a result of the stability of the nano-scale filler in the comoposite. Both single-walled (SWNT) and multi-walled carbon nanotubes (MWNT) have been assimilated into various polymeric matrices. For example, carbon nanotubes have been incorporated into the matrices of conjugated polymers, such as poly(phenylenevinylene) and polythiophene, as composite materials useful for optoelectronic applications.[2-5] Carbon nanotubes have also been used as fillers in epoxy resin to take advantage of the superior mechanical properties of the nanotubes. However, several issues concerning the dispersion of carbon nanotubes in the polymer matrices and the effects on the properties of the resulting nanocomposite materials remain to be addressed.

Polystyrene (PS) is one of the most widely used commercial polymers. Many researchers have interest in the dispersion of carbon nanotubes into PS matrix for the fabrication of PS-carbon nanocomposites.[6-10] Qian *et al.* reported the fabrication of PS/MWNT nanocomposites using ultrasonication in toluene.[6,7,11] A drastic increase in the elastic modulus and break stress in the PS/MWNT nanocomposite containing 1 wt. % nanotube was reported. The mechanical properties of a

polypropylene-carbon fiber (10 wt. %) composite was also studied.[6,7,11] These results are in general agreement with the prediction from a theoretical study of nonbonding PS-carbon nanotube composite system.[9] Watts *et al.* used a similar ultrasonication method to prepare PS composites with various carbon materials, including MWNTs and boron-doped MWNTs, and studied the conductivity in these composites.[10] The study proposed that the conducting networks in the PS/MWNT composites were built upon the nanotube-nanotube bundling and crossing, which were responsible for the relatively low resistance in the materials. However, the generally poor compatibility between PS and MWNT bundles was a problem with the nanocomposites due to an inhomogeneous dispersion of MWNTs in the PS matrix. The nanotubes settle to the bottom in a PS-MWNT film, resulting in localized conductivity changes.[10] It is widely acknowledged that the quality of nanocomposites depends on the dispersion of carbon nanotubes in the polymer matrices.

In this paper, we report the well-dispersed morphology of bulk PS/MWNT nanocomposites prepared by co-rotating twin-screw extrusion because this method can be applied to industry directly. Indeed, the influence of the nanotube content on the T_gs and thermal stability will be discussed.

Experimental

Materials

The PS used in this study was acquired from LG Chemical. Ltd.(Seoul, Korea) and was used as obtained. The weight-average molecular weight is 59,000 (PDI = 1.98). The MWNT were obtained from Illjin Nanotech Co., Ltd. (Seoul, Korea). The typical dimensions of the MWNT are 10-20 nm in diameter and about 10-50 μm in length.

Preparation of nanocomposites

The nanocomposites were prepared with a co-rotating, intermeshing, twin-screw extruder (Lapman-20, Shinsung Platech. Co., Ltd., Bucheon, Korea) with a screw diameter of 20 mm, a length-to-diameter ratio (L/D) of 32, a die diameter of 3.5 mm, and a screw speed of 50 rpm. The temperature profile was 190-210-200℃, representing the temperatures at the hopper zone, three barrel zones, and heating zone in the die head, respectively. The extruded strand was immediately quenched in a water bath and dried in a vacuum oven.

Characterization and measurements

The thermal characterization studies were conducted using a Mettler-Toledo, DSC882e, in which the heating rate was 10 ℃/min. TGA was performed with a Mettler-Toledo, TG 50 thermal analysis system, in which the TGA scans were recorded at 10 ℃/min under a N_2 atmosphere from 30 to 600 ℃. Ultrathin sections of nanocomposite with a thickness of approximately 50 nm were prepared with an ultramicrotome (Leica Reichert; Ultracut S/FC S) equipped with a diamond knife. The structural morphology of the nanocomposite was observed using transmission electron microscopy (TEM; FEI; Tacnai 12) at an acceleration voltage of 120 kV and

field emission scanning electron microscopy (FE-SEM; Jeol; JSM-6700F) at an acceleration voltage of 5 kV. An Advanced Rheometric Expansion System (ARES, Rheometric Scientific) with a parallel-plate fixture (25 mm diameter) was used to conduct dynamic frequency sweep experiments (ranging from 0.01 to 100 rad/sec) at 180, 200, and 220 ^{o}C.

Results and discussion

The color of PS/MWNT nanocomposite produced by twin-screw extrusion was black, even though the MWNT was added 1 wt.% amount. The morphologies of carbon nanotube filled PS were investigated by SEM and TEM. Figure 1 shows four FE-SEM photomicrographs of the PS/MWNT nanocomposites containing 1, 3, 5, and 7 wt.% of MWNT, respectively. The MWNT used in this study exhibited a distinct curved shape in all three dimensions, as a result of interlocking between the MWNT (Fig. 1 C). A similar kind of interlocked structure has been reported in poly(vinyl alcohol)/MWNT composites at 50 wt. % MWNT content.[12] Figure 1 (A), 1 (B) and 1(D) show that the structure and shape of the nanotubes are randomly oriented.

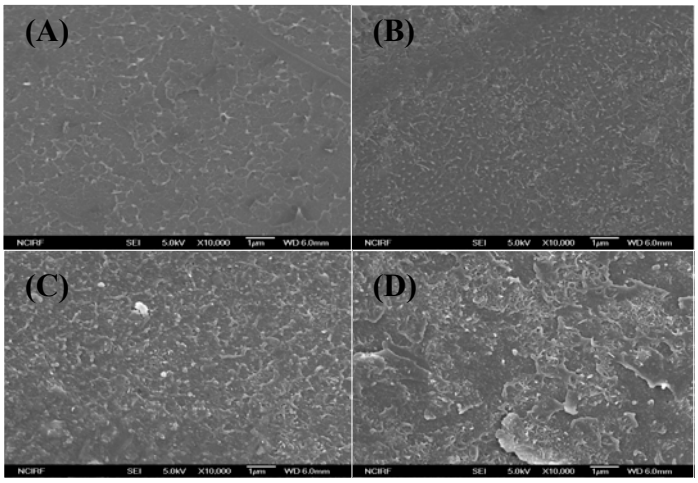

Figure 1. SEM photomicrographs of PS/MWNT nanocomposites; (A) MWNT 1 wt.%, (B) 3 wt.%, (C) 5 wt.%, (D) 7 wt.%.

Figure 2 shows TEM photomicrographs of PS/MWNT nanocomposites, cut perpendicular to the extrusion direction, containing 1, 3, 5, and 7 wt. % of MWNT, respectively. The distribution of MWNT is almost homogeneous at all concentration. The individual nanotubes are uniformly distributed in the PS matrix without agglomeration of clusters, and are recognizable as long hollow fibers with a diameter of 15-20 nm. Only very small areas of enhanced carbon density can be observed which is likely as result of amorphous carbon parts or catalytic impurities in the nanotube material. Previous studies reported that nanotubes can align by flow induced orientation in nanotube/surfactant solutions and also in polymer-nanotube nanocomposites. MWNT may also align in drawn monofilament composite fibers of PC/MWNT.[13] There are expectations that nanotubes can be easily oriented by shear. On the other hand, there are assumptions that MWNT do not orient during melt

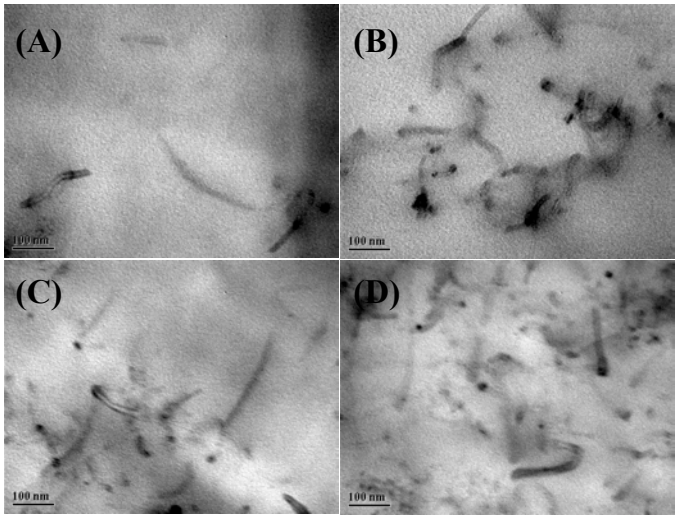

Figure 2. TEM photomicrographs of PS/MWNT nanocomposite; (A) MWNT 1 wt.%, (B) 3 wt.%, (C) 5 wt.%, (D) 7 wt.%.

processes due to their size and geometry. In order to obtain conductivity at low nanotubes contents, a random distribution should be favorable. In order to exploit the mechanical potential of carbon nanotubes, a preferential orientation is desired. If preferential orientation of the nanotubes occurred as a result of the extrusion process, TEM micrographs of cuts/sections made perpendicular to the orientation of the MWNT would show circular discs. As shown in Figure 2, a preferred orientation is not observed in our case. Therefore, the nanotubes are oriented in all directions. We suggest the random nanotube orientation is caused; *i*) by the high aspect ratio, *ii*) by the flexibility and winding shape of original nanotube, and *iii*) by the high matrix viscosity.

The frequency sweep tests at a processing temperature of PS were conducted, as rheological experiments are another sensitive tool to investigate the dispersion of the filler in a viscoelastic fluid. Figure 3 shows log G′ vs. log G″ plot for pure PS and PS/MWNT nanocomposite (95/5; wt/wt) at 180, 200 and 220 ℃. It has been amply demonstrated that a log G′ vs. log G″ plot is independent of temperature for homogeneous polymers and also for heterogeneous polymer systems as long as the morphological state does not vary with temperature.[14] In this regard, the log G′ vs. log G″ plot may be used very effectively to determine whether or not the morphological state of a multiphase polymer system varies with temperature.[15,16] As shown in Figure 3, the log G′ vs. log G″ plot for pure PS is independent of temperature, but its slope in the terminal region is slightly less than 2. It has been pointed out earlier [17] that the slope of log G′ vs. log G″ plots for monodisperse polymers is expected to be 2 only if the applied frequency is sufficiently low (much lower than 0.01 rad/sec applied in the present study). Therefore, this observation is not surprising due to the broad molecular weight distribution (PDI =1.98) of PS. However, we observed that at G′ < 1000 Pa the log G′ vs. log G″ plots of PS/MWNT nanocomposite are shifted upward by about 1 order of magnitude from those of pure PS, and at G′ > 1000 Pa the log G′ vs. log G″ plots of the nanocomposite have a very small slope, exhibiting solid-like behavior. The plots of

the nanocomposite (Figure 3) show the slope shifted upward as the temperature increased from 180 to 220 ℃. The temperature dependence of log G′ vs. log G″ plots observed in Figure 3 for PS/MWNT nanocomposite is similar to that observed in Han's work[18] for polymer-clay nanocomposites. Although the magnitude of upward shift is small, compared to that observed in Han's works, it is indicative of an increase in the surface area as a result of enhanced dispersion of MWNT aggregates with increasing temperature.

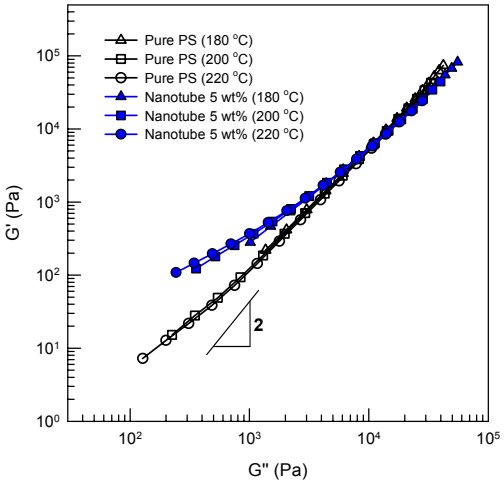

Figure 3. Plot of log G′ vs. log G″ for PS/MWNT nanocomposite and pure PS at 180, 200 and 220 ℃.

Figure 4 shows the linear viscoelastic dynamic moduli of PS/MWNT nanocomposites at 200 ℃ as functions of frequency. We observed a small effect of the MWNT on the G′ of PS/MWNT nanocomposite; namely, adding MWNT increased the values of G′ of PS/MWNT nanocomposite in the low frequency region (Figure 4a). The PS/MWNT nanocomposite exhibited solid-like behavior, in contrast to the pure PS. We also observed a pronounced effect of the MWNT on the G″ of PS/MWNT nanocomposite; in the low frequency region values of G″ for the PS/MWNT nanocomposite are more than those of pure PS (Figure 4b). The increase of G′ at low value of frequency observed in Figure 4a is attributable to the increased surface area due to an enhanced dispersion. That is, when the MWNT aggregates are better dispersed in the polymeric matrix, the surface area of MWNT is expected to markedly increase.

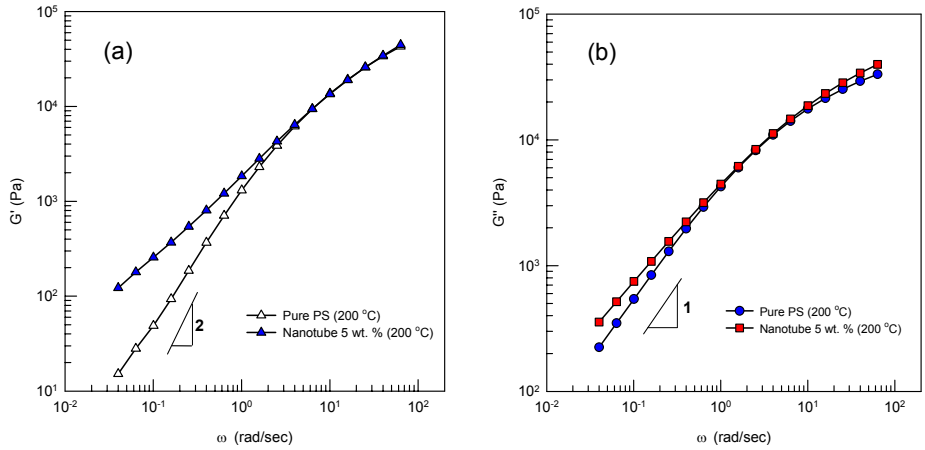

Figure 4. Plot of (a) log G′ vs. log ω and (b) log G″ vs. log ω for PS/MWNT nanocomposite and pure PS at 200 ℃.

Table 1. Glass transition temperatures and Kinetic parameters[§] of thermal degradation for PS/MWNT nanocomposites under nitrogen.

	T_g (℃)	T_d [a] (℃)	E (KJ/mol)	n	r_1 [b]	r_2 [b]	Ln(Z) (min^{-1})
Pure PS	90	382	168 (±1.7)	7.5 (±0.1)	0.99908	0.99755	22.6
MWNT-1wt.%	91	382	196 (±1.9)	5.4 (±0.1)	0.99837	0.99343	28.1
MWNT-3wt.%	96	398	205 (±2.0)	5.3 (±0.1)	0.99757	0.99525	29.1
MWNT-5wt.%	98	401	193 (±2.0)	4.2 (±0.1)	0.99935	0.99838	26.4
MWNT-7wt.%	99	405	175 (±1.8)	2.5 (±0.1)	0.99659	0.99938	23.7

[a]: 5 % weight loss temperature

[b]: The symbol, r, is the linear correlation coefficient, and r_1 and r_2 are correspondent to Ln(dα/dt) vs. $1/T$ and Ln(1-α) vs. $1/T$, respectively.

[§] The kinetics parameters were calculated in the temperature range from [T_d – (10~40)K] to T_d, in which the linear relation between Ln(dα/dt) and $1/T$ is available.

The glass transition temperatures are summarized in Table 1. The nanocomposites in the bulk exhibit higher Tg's than the pure PS sample. Although there is no chemical bonding between MWNT and PS matrix, Liao *et al.*[19] reported the interfacial characteristics of a carbon nanotube (CNT)-reinforced PS composite system through molecular mechanics simulations and elasticity calculations. Their results show that the adhesion of CNT-PS system comes from *i*) electrostatic and van der Waals interaction, *ii*) mismatch item n coefficient of thermal expansion (CTE), and *iii*) radial deformation induced by atomic interaction. Therefore, if the motion of PS chains can be restricted by the adhesion of PS/MWNT, the Tg of PS should increase with increasing the MWNT content.

The thermal stability of PS/MWNT is slightly improved by the incorporation of MWNTs (Fig.5). The onset of degradation is delayed by 7 ℃ upon the incorporation of 7 wt. % of MWNT. The improved thermal stability of the nanocomposite may come from the enhanced distribution of MWNT raising the surface area in the polymer matrix.

To investigate the thermal decomposition kinetics, we calculated the kinetic parameters of the pure PS and PS/MWNT nanocomposites by using the Friedman single heating-rate method.[20] The decomposition kinetics of organic materials is attributed to the kinetic equation:

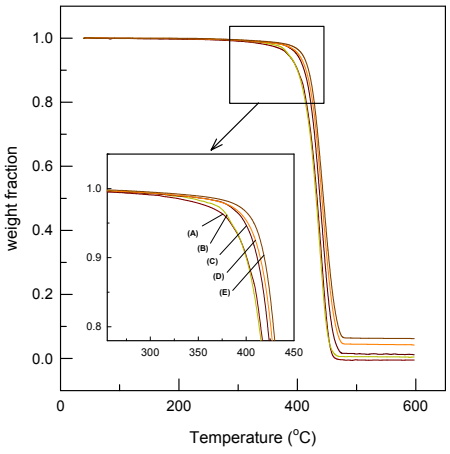

Figure 5. TGA thermograms for PS/MWNT nanocomposite; (A) pure PS, (B) MWNT 1 wt.%, (C) 3 wt.%, (D) 5 wt.%, (E) 7 wt.%.

$$d\alpha/dt = Z \cdot (1-\alpha)^n e^{-E/RT} \qquad (1)$$

where α is the weight loss of the polymer undergoing degradation at time *t*, dα/d*t* denotes the decomposition rate or weight-loss rate, *Z* is the frequency factor, *n* represents the decomposition reaction order, *E* stands for the activation energy, *R* is the gas constant (8.3136 J·mol^{-1}·K^{-1}), and *T* symbolizes the absolute temperature (K).[21] The Friedman technique is one of the single heating-rate methods used with thermogram and differential thermogravimetry (DTG) data to find the kinetic parameters of thermal decomposition; it is expressed by equation (2)

$$\mathrm{Ln}(Z) = \mathrm{Ln}(d\alpha/dt) - n \cdot \mathrm{Ln}(1-\alpha) + E/RT \qquad (2)$$

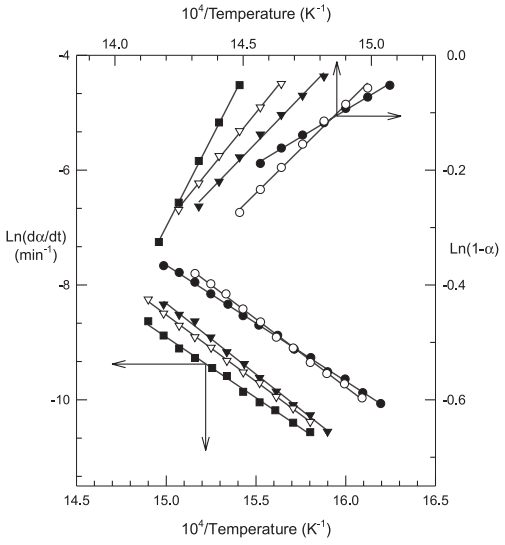

Figure 6. Friedman plots of Ln(*dα/dt*) or Ln(1-α) vs. 1/*T* for the direct calculation of *E* and *n* of thermodegradation; (●) pure PS, (○) MWNT 1 wt.%, (▼) 3 wt.%, (▽) 5 wt.%, (■) 7 wt.%.

which is the natural logarithmic differential form of Eq. (1). From a plot of Ln(dα/d*t*) or Ln(1-α) against *1/T* for each sample, the value of *–E/R* or *E/(nR)* was determined from the slope, after which *Z* could be calculated from Eq. (1).[20]

Figure 6 shows the relationship given by Eq. (2) of Friedman technique and the resulting kinetic parameters together with their error ranges; the linear correlation coefficients are summarized in Table 1. In general, the activation energy (*E*) corresponds to the lowest energy needed for reaction (degradation). Thus, a high *E* value indicates high inertness (*i.e.*, thermostability). Additionally, *n* indicates the exponential relation between the concentration of reactant (1-α) and the weight-loss rate (d*α*/d*t*) described in Eq. (1). Therefore, the large *n* value indicates a low degradation rate.[22] From Table 1, it can be concluded that the kinetic parameters change with MWNT content. The activation energies of PS/MWNT nanocomposites are bigger than that of pure PS. However, the reaction orders of them are decreased with increasing the MWNT content. It indicated that the PS/MWNT nanocomposites have higher inertness than pure PS, but its degradation rate at a higher temperature is faster than that of pure PS.

Conclusions

From the microscopic investigations (SEM and TEM), the nanotubes are dispersed uniformly in the PS/MWNT nanocomposites prepared by twin-screw extrusion with no evidence of segregation to the surface of the extruded strand and without preferred

alignment. Rheometer is another technique, which can also be used to get information about the state of nanotube dispersion indirectly. The rheological investigation conducted in this study showed that the morphology of MWNT nanocomposites may be temperature dependent as determined from the temperature dependence of log G′ vs. log G″ plots due to the change of surface area. Therefore, the rheological measurement should be applied to characterize the dispersion on polymer-MWNT nanocomposites qualitatively. The bulk Tg, as determined by DSC, of the PS/MWNT nanocomposites is increased with increasing the MWNT content. This result emphasizes the influence PS and MWNT interaction on the Tg of the nanocomposite. The thermal stability of PS/MWNT nanocomposites also increased due to increasing the surface area of MWNT on the PS matrix.

Acknowledgement. This research was supported by a grant from the Center for Advanced Materials Processing (CAMP) of the 21st Century Frontier R&D Program funded by the Ministry of Science and Technology, Republic of Korea.

References

1. Thostenson ET, Ren Z, Chou T-W (2001) Comp Sci Tech 61:1899
2. Ajayan PM (1999) Chem Rev 99:1787
3. Ago H, Petritsch K, Shaffer MSP, Windle AH, Friend RH (1999) Adv Mater 11:1281
4. Curran SA, Ajayan PM, Blau WJ, Carroll DL, Coleman JN, Dalton AB, Davey AP, Drury A, McCarthy B, Maier S, Strevens A (1998) Adv Mater 10:1091
5. Star A, Stoddart JF, Steuerman D, Diehl M, Boukai A, Wong EW, Yang X, Chung SW, Choi H, Heath JR (2001) Angew Chem, Int Ed 40:1721
6. Qian D, Dickey EC, Andrews R, Rantell T (2000) Appl Phys Lett 76:2868
7. Qian D, Dickey EC (2001) J Microsc 204:39
8. Safadi B, Andrews R, Grulke EA (2002) J Appl Polym Sci 84:2660
9. Liao K, Li S (2001) Appl Phys Lett. 79:4225
10. Watts PCP, Hsu WK, Chen GZ, Fray DJ, Kroto HW, Walton DRM (2001) J Mater Chem 11:2482
11. Grimes CA, Dickey EC, Mungle C, Ong KG, Qian D (2000) J Appl Phys 90: 4134
12. Shaffer MSP, Windle AH (1999) Adv Mater 11:937
13. Sennett M, Welsh E, Wright JB, Li WZ, Wen JG, Ren ZF (2003) Appl Phys A 76:111
14. Han CD, Jhon MS (1986) J Appl Polym Sci 32:3809
15. Kim SS, Han CD (1993) Macromolecules 26:3176
16. Han CD, Beak DM, Kim JK (1990) Macromolecules 23:561
17. Han CD, Kim JK (1989) Macromolecules 22:4292
18. Lee KM, Han CD (2003) Macromolecules 36:804
19. Liao K, Li S (2001) Appl Phys Lett 79:4225
20. Friedman HL (1964) J Polym Sci: Part C 183
21. Li X-G, Huang M-R, Guan G-H, Sun T (1998) Polym Int 46:289
22. Hwang S-H, Yoo KS, Moorefield CN, Lee S-W, Newkome GR (2004) J Polym Sci, Part B: Polym Phys 42:1487